*J. Fluid Mech.* (2002), *vol.* 451, *pp.* 283–294.  
DOI: 10.1017/S0022112001006528 Printed in the United Kingdom

# Inclined turbulent fountains

By LYNN J. BLOOMFIELD AND ROSS C. KERR

Research School of Earth Sciences, The Australian National University, Canberra, ACT 0200, Australia

(Received 2 April 2001 and in revised form 22 June 2001)

We present an experimental investigation of turbulent fountains produced when dense fluid is injected upwards into either a homogeneous or a stratified environment at an angle to the vertical. We determine the initial height above the source at which the flow first comes to rest, the final height of the fountain, and the height at which the mixed fluid finally intrudes when the environment is stratified. The initial fountain height is found to decrease monotonically as the angle of inclination is increased. In contrast, the final fountain height is found to increase and then to decrease, with the maximum height occurring at an angle of inclination of about 10°. This behaviour is due a combination of the decreased interaction between the upflow and the downflow, and the decreased vertical momentum of the injected fluid, as the angle of inclination is increased.

## 1. Introduction

Turbulent fountains are formed when a continuous jet of dense fluid is injected rapidly upwards into a less dense environment, or when a continuous jet of buoyant fluid is injected rapidly downwards into a denser environment (Turner 1966). They arise in a number of important situations both in engineering and in nature, including the forced heating or cooling of aircraft hangers, buildings or rooms (Baines, Turner & Campbell 1990), the disposal of brines, sewerage and industrial waste into the ocean (Koh & Brooks 1977), the improvement of water quality by forced mixing in reservoirs, small lakes and harbours (Larson & Jönsson 1994; McClimans & Eidnes 2000), vehicle exhausts and accidental leaks of hazardous gases (Lane-Serff, Linden & Hillel 1993), the evolution of volcanic eruption columns (Woods & Caulfield 1992), the replenishment of magma chambers in the Earth's crust (Turner & Campbell 1986; Campbell & Turner 1989), and the exit snow from snowploughs (Lindberg & Peterson 1991).

Motivated by these diverse applications, the dynamics of turbulent fountains has been explored in a number of experimental and theoretical studies over the past twenty years (e.g. Fischer *et al.* 1979; McDougall 1981; Mizushina *et al.* 1982; Baines *et al.* 1990; Lindberg & Peterson 1991; Lane-Serff *et al.* 1993; Lindberg 1994; Bloomfield & Kerr 1998, 1999, 2000). In particular, extensive investigations have been made of both axisymmetric and two-dimensional fountains in homogeneous environments (Baines *et al.* 1990), in stratified environments (Bloomfield & Kerr 1998), and in environments with confining boundaries (Baines *et al.* 1990; Bloomfield & Kerr 1999). However, there has been relatively little examination of the effect of the angle of inclination of the source on the behaviour of turbulent fountains, despite its likely importance in many industrial and natural applications (Fischer *et al.* 1979; Baines *et al.* 1990).

Some experimental observations of an axisymmetric fountain inclined at an angle

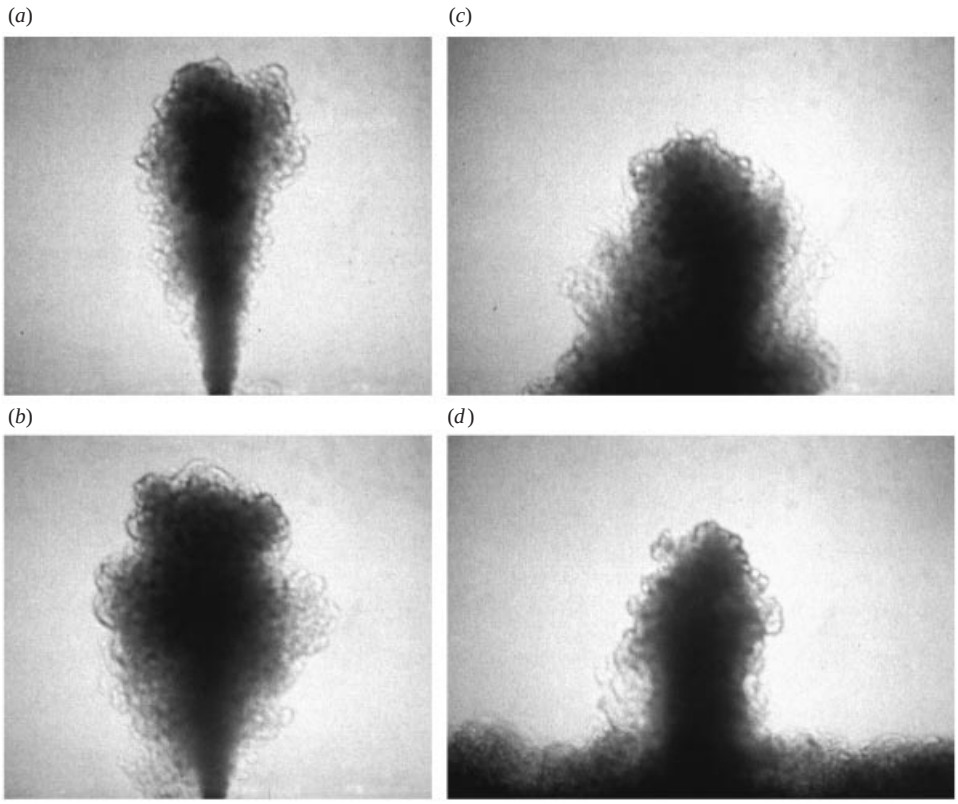


FIGURE 1. Photographs of a vertical axisymmetric turbulent fountain as a function of time. (*a*) The initial upflow is jet-like. (*b*, *c*) The downward buoyancy force brings the fluid to rest at an initial maximum height, before it falls as an annular plume surrounding the upflow. (*d*) The turbulent interaction between the upflow and downflow produces a final height of the fountain that is smaller than its initial height.

of 7° to the vertical in a homogeneous fluid were reported by Baines *et al.* (1990). They made the important discovery that the final height of their inclined fountain was about 17% larger than for a vertical fountain with the same source conditions, and that the entrainment from the environment at all elevations was about 40% larger. In contrast, experiments by Lane-Serff *et al.* (1993) at angles of 15° to 75° in a homogeneous fluid produced fountains with final heights that decreased monotonically with increasing inclination angle. In this paper, our aim is to build on these past observations by systematically explorating the effect of inclination angle on the height of turbulent fountains, in both homogeneous and stratified environments. In particular, we will determine the inclination angle that results in the maximum fountain height. In § 2, we describe our experimental investigations of inclined turbulent fountains in a homogeneous fluid. Then, in § 3, we explore inclined turbulent fountains in a stratified fluid. Our conclusions are summarized in § 4.

## 2. Inclined fountains in a homogeneous fluid

### 2.1. *Past work*

The behaviour of an axisymmetric turbulent fountain produced by a vertical source in a homogeneous fluid has been extensively investigated (Turner 1966; Mizushina

*et al.* 1982; Baines *et al.* 1990; Bloomfield & Kerr 2000). As shown in figure 1, the flow rises initially as a jet, entraining surrounding fluid and thereby decreasing its density. The momentum of the rising fluid is reduced by the opposing buoyancy force until the flow comes to rest at an initial height above the source (figure 1*a*). The downflow which forms after this point continues to mix with the environment while also interacting turbulently with the upflow (figure 1*b*, *c*). This interaction restricts the rise of subsequent fluid and therefore reduces the initial fountain height to a final value (figure 1*d*), about which there are random fluctuations of order 10% of the fountain height. Bloomfield & Kerr (2000) determined experimentally the initial, $z_i$, and final, $z_f$, fountain heights as a function of the momentum flux and buoyancy flux at the source:

$$\left.\begin{aligned} z_i &= (2.32 \pm 0.08) M_o^{3/4} F_o^{-1/2}, \\ z_f &= (1.70 \pm 0.17) M_o^{3/4} F_o^{-1/2}, \end{aligned}\right\} \tag{2.1}$$

where the momentum flux at the source, $M_o$, and the buoyancy flux at the source, $F_o$, are defined by

$$\left.\begin{aligned} M_o &= \pi r_e^2 U_o^2 = Q_o^2/\pi r_e^2, \\ F_o &= \pi r_e^2 U_o \Delta_o = \Delta_o Q_o. \end{aligned}\right\} \tag{2.2}$$

In these expressions, $r_e$ is the effective source radius, $U_o$ is the velocity of the source fluid, $\Delta_o = (g/\rho_o)(\rho_i - \rho_o)$, $g$ is the gravitational acceleration, $\rho_o$ is the density of the ambient fluid, $\rho_i$ is the density of the source fluid and $Q_o = \pi r_e^2 U_o$ is the volume flux of source fluid. The effective source radius, $r_e$, is determined experimentally, and depends on whether the source fluid is laminar or turbulent on entering the environment (Baines *et al.* 1990; Bloomfield & Kerr 1999). For fully laminar flow, $r_e = \sqrt{3} r_o/2$, while for turbulent flow, $r_e = r_o$, where $r_o$ is the measured source radius.

### 2.2. *Experimental method*

The experiments were carried out in an acrylic tank of internal dimensions 38 cm × 38 cm and 80 cm deep (this is the same tank as used by Bloomfield & Kerr 1998, 1999 for previous fountain experiments). The source fluid was placed in a 20 l bucket which was raised about 1 m higher than the main tank. The flow rate resulting from this gravitational head was adjusted with a valve and measured with a flow meter to an accuracy of about 1%.

The source fluid was injected upwards from the base of the tank through one of two different tubes. In the first tube, which had an 8.8 mm inner diameter, a set of 0.5 mm diameter crosswires was positioned 3 mm from the tube outlet with a second set placed 44 mm further along the tube, to ensure that the flow from this source was turbulent on entering the environment. In previous experiments by Bloomfield & Kerr (1998, 1999) using the same source and source conditions, it was determined that the virtual source was a distance $z_v = 1.0 \pm 0.25$ cm below the end of the tube, and that the effective source radius was $r_e = 4.16 \pm 0.23$ mm. In the second tube, which had an 3.16 mm inner diameter and no crosswires, the virtual source was found to be at the end of the tube and the effective source radius was $r_e = 1.47 \pm 0.08$ mm.

To produce an inclined fountain, both the tank and source were tilted at the desired angle. The flows were observed using the shadowgraph method and were recorded on video. This procedure allowed the initial fountain height to be measured to within 2–3%, and the mean final fountain height to be measured to within 4–6% (with the latter error being greater due to greater turbulent fluctuations in the final fountain height).

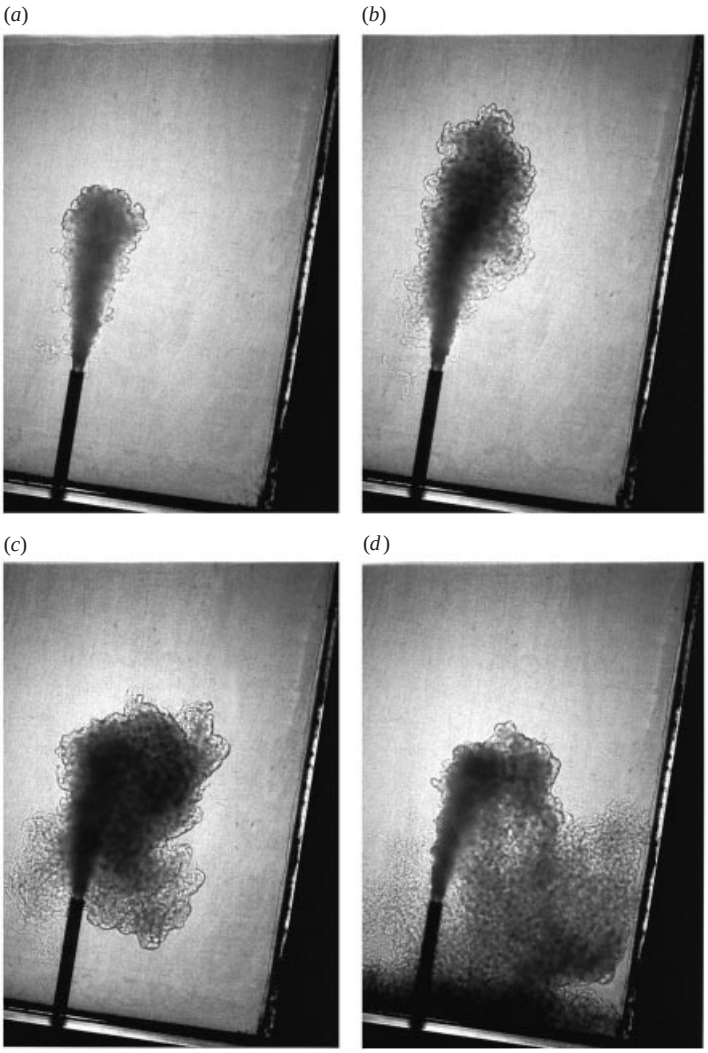


FIGURE 2. Photographs of a turbulent axisymmetric fountain formed from a source inclined at 10° to the vertical. (*a*) The initial flow is jet-like. (*b*) The downward buoyancy force brings the fluid to rest at an initial maximum height. (*c*, *d*) The fluid then falls as a plume and partially interacts with the upflow, resulting in smaller final height of the fountain.

### 2.3. *Experimental results*

A total of 33 experiments were performed at angles between 0° and 60° to the vertical. Figure 2 shows the evolution of a fountain inclined at 10°. The initial upflow is jet-like (figure 2*a*), before the flow comes to rest at an initial maximum height (figure 2*b*). The flow then falls down and partially interacts with the the upflow, producing a smaller final fountain height (figure 2*c*, *d*). It is clear, however, that the turbulent interaction between the upflow and downflow is much smaller than that for a vertical fountain (cf. figure 1).

Our measurements of the dimensionless initial height ($\tilde{z}_i = z_i M_o^{-3/4} F_o^{1/2}$) are plotted against inclination angle $\theta$ in figure 3. Also shown in figure 3 is a curve of the form $\tilde{z}_i \propto \cos^{3/4}\theta$ proposed by Fischer *et al.* (1979), based on the argument that the fountain

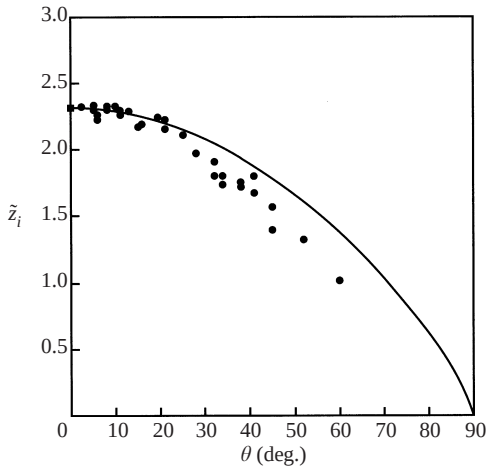


FIGURE 3. Dimensionless initial fountain height $\tilde{z}_i$ as a function of the source inclination angle $\theta$. Also shown is the mean initial height of a vertical fountain (■), from Bloomfield & Kerr (2000). The curve shows the equation $\tilde{z}_i = 2.32\cos^{3/4}\theta$.

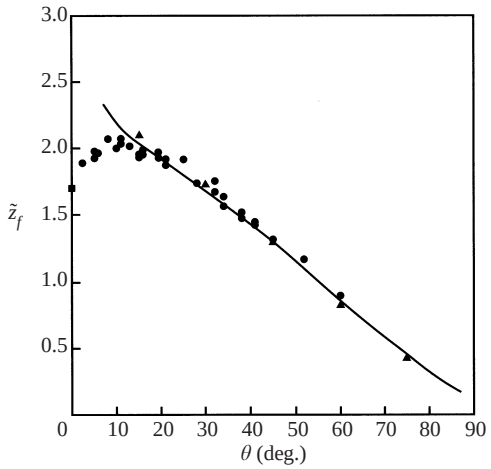


FIGURE 4. Dimensionless final fountain height $\tilde{z}_f$ as a function of the source inclination angle $\theta$: ■, Bloomfield & Kerr (2000); ▲, Lane-Serff *et al.* (1993); ●, the present study. The curve shows the height predicted by a theoretical model of forced, angled plumes developed by Lane-Serff *et al.* (1993).

height depends on the buoyancy flux at the source $F_o$ (as in a vertical fountain) and on the vertical component of the momentum flux at the source $M_o\cos\theta$. It is seen that $\tilde{z}_i$ decreases monotonically with increasing $\theta$, but at a rate that is more rapid than the theoretical estimate of Fischer *et al.* (1979).

In figure 4, our measurements of the dimensionless final height ($\tilde{z}_f = z_f M_o^{-3/4} F_o^{1/2}$) are plotted against $\theta$, together with five experiments by Lane-Serff *et al.* (1993). At small inclination angles, $\tilde{z}_f$ is found to increase rapidly with increasing angle, as discovered by Baines *et al.* (1990). This behaviour reflects the rapid decrease in the turbulent interaction between the upflow and downflow as the inclination angle is increased. At large inclination angles, $\tilde{z}_f$ is found to decrease almost linearly with increasing $\theta$, due to the decreased vertical momentum flux at the source and

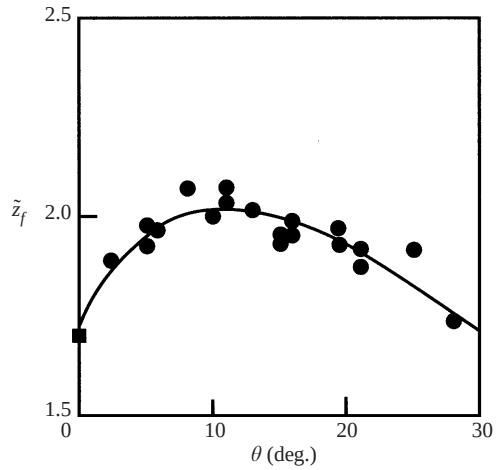


FIGURE 5. Dimensionless final fountain height $\tilde{z}_f$ as a function of the source inclination angle $\theta$, for angles between 0° and 30°: ■, Bloomfield & Kerr (2000); ●, the present study. The curve shows a polynomial fit to the data ($\tilde{z}_f = 1.73 + 6.50 \times 10^{-2}\,\theta - 4.61 \times 10^{-3}\,\theta^2 + 1.24 \times 10^{-4}\,\theta^3 - 1.69 \times 10^{-6}\,\theta^4 + 9.04 \times 10^{-9}\,\theta^5$).

the increased entrainment along the curved path of the fountain. Between these two regimes, at an angle of about 10°, the dimensionless fountain height reaches a maximum of $2.05 \pm 0.05$, which is about 20% higher than the height of a vertical fountain (see also figure 5).

Also shown in figure 4 is a curve giving the predictions of a simple theoretical model for inclined plumes and fountains that was developed by Lane-Serff *et al.* (1993). Their theoretical model is based on the entrainment assumption (Morton, Taylor & Turner 1956; Turner 1973) and on the conservation of mass, density, horizontal momentum, and vertical momentum. As figure 4 shows, the model predictions are in excellent agreement with the laboratory experiments for inclination angles greater than about 15°. However, at smaller angles, the model predictions diverge from the experimental observations as the separation between the downflow and the upflow is lost, the upflow and downflow begin to entrain each other as well as the stationary ambient fluid (see figure 2), and the theoretical model becomes invalid (see figure 15 of Lane-Serff *et al.* 1993).

## 3. Inclined fountains in a stratified fluid

### 3.1. *Past work*

The behaviour of an axisymmetric turbulent fountain produced by a vertical source in a linearly stratified fluid was investigated by Bloomfield & Kerr (1998). They determined the initial and final heights of the fountain as a function of the strength of the stratification, using the dimensionless parameter $\sigma = M_o^2 N^2 / F_o^2$, where $N = (-(g/\rho_o)(\mathrm{d}\rho/\mathrm{d}z))^{1/2}$ is the buoyancy frequency and $\rho(z)$ is the ambient density at a height $z$ above the base of the tank. Bloomfield & Kerr also found that, if the stratification is sufficiently strong ($\sigma > 5.0$), the flow intrudes at an intermediate height, $z_s$, in the environment rather than spreading along the base of the tank. They also observed that the ratio of the initial to final fountain height becomes smaller as the stratification becomes stronger, due to a decrease in the turbulent interaction between the upflow and the downflow. Finally, in the limiting case of zero buoyancy flux at the source (i.e. $F_o = 0$, and hence $\sigma = \infty$), Bloomfield & Kerr (1998) experimentally

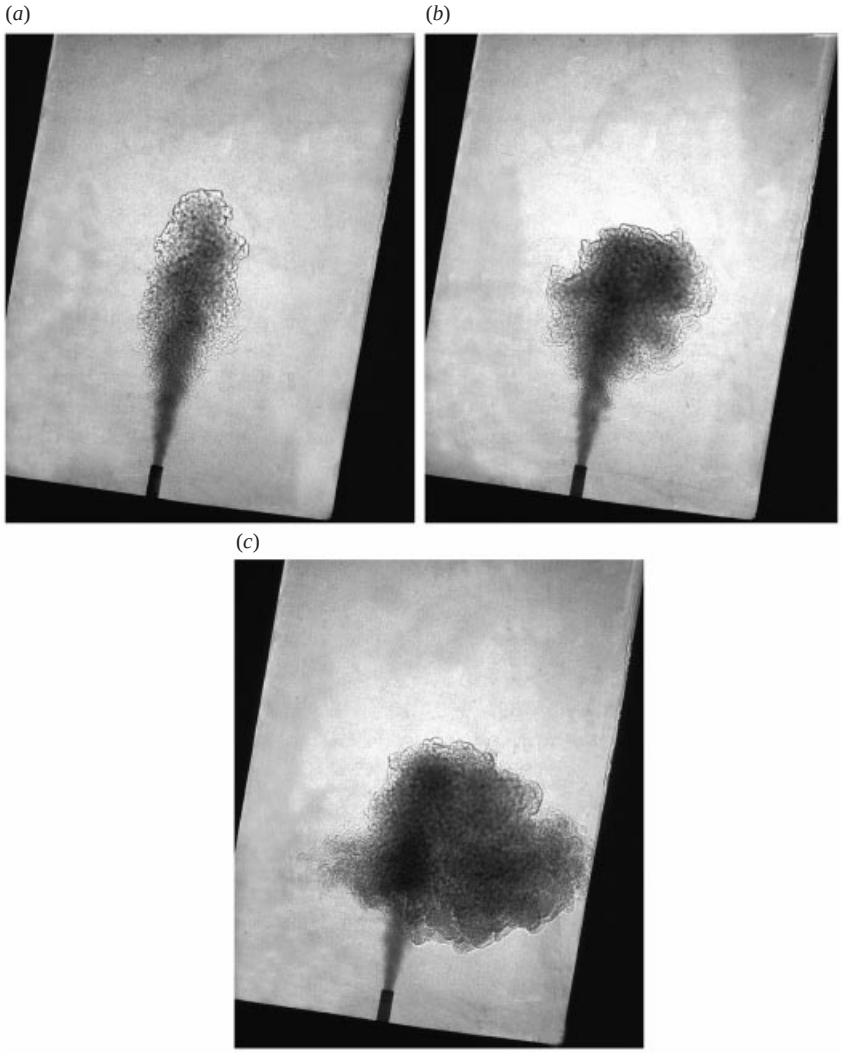


FIGURE 6. Photographs of a turbulent axisymmetric fountain in a stratified fluid, formed from a source inclined at 10° to the vertical. (*a*) The initial flow is jet-like as the fluid rises to an initial maximum height. (*b*) The fluid then falls as a plume and partially interacts with the upflow, resulting in smaller final height of the fountain. (*c*) The fountain fluid becomes neutrally buoyant and intrudes into the stratified fluid at an intermediate spreading height.

determined expressions for the initial, final and spreading heights of the fountain:

$$\left.\begin{aligned} z_i &= (3.25 \pm 0.17) M_o^{1/4} N^{-1/2}, \\ z_f &= (3.00 \pm 0.23) M_o^{1/4} N^{-1/2}, \\ z_s &= (1.53 \pm 0.10) M_o^{1/4} N^{-1/2}. \end{aligned}\right\} \tag{3.1}$$

### 3.2. *Experimental method*

In investigating the effect of source inclination on turbulent fountains in a stratified fluid, we focused on small angles of inclination, given the existence of theoretical models (see Schatzmann 1978; Hofer & Hutter 1981*a*) which accurately describe the

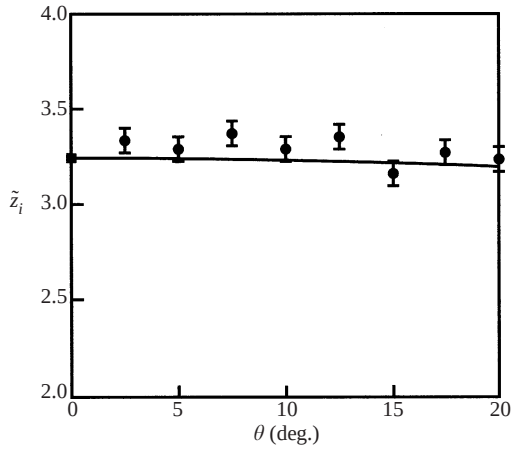


FIGURE 7. Dimensionless initial height of a turbulent fountain in a stratified fluid as a function of the source inclination angle $\theta$. Also shown is the mean initial height for a vertical fountain (■), from Bloomfield & Kerr (1998). The curve shows the equation $\tilde{z}_i = 3.25\cos^{1/4}\theta$.

behaviour of turbulent fountains in a stratified fluid when there is no interaction between the upflow and the downflow (Hofer & Hutter 1981*b*).

The experiments used the tank, the first source tube and the flow visualization procedures described in § 2.2. Linear density gradients were established with NaCl solutions using the double bucket method (Oster 1965). The density gradient was determined, to within 2%, from measurements of the refractive index at various heights in the tank. The position of the source was then adjusted until it was at the level at which the ambient density was equal to that of the source fluid. We also note that the source in our experiments was always at a height that was above the highest part of the base (e.g. see figure 6), which ensured that the cross-sectional area of the tank was constant, and hence the density gradient in the tank was linear, at all heights above the source. In these experiments, the measurement errors were about 2% for the initial fountain height, about 3% for the mean final fountain height, and about 6% for the spreading height.

### 3.3. *Experimental results*

#### 3.3.1. *Zero buoyancy flux at the source*

For the limiting case of zero buoyancy flux at the source ($\sigma = \infty$), a total of eight experiments were performed at angles between 0° and 20° to the vertical. The qualitative behaviour observed (figure 6*a*, *b*) was similar to that shown in figure 2 for a homogeneous environment, except that the downflow only falls about halfway down before it becomes neutrally buoyant. At this point, the flow still has some downward momentum, so a small overshoot is observed before it intrudes into the environment (figure 6*c*).

Our measurements of the dimensionless initial height ($\tilde{z}_i = z_i M_o^{-1/4} N^{1/2}$) are plotted against inclination angle $\theta$ in figure 7. Also shown in figure 7 is a curve of the form $\tilde{z}_i \propto \cos^{1/4}\theta$, which is based on the argument (cf. § 2.3) that the fountain height only depends on the buoyancy frequency $N$ and on the vertical component of the momentum flux at the source $M_o \cos\theta$. There is little decrease in $\tilde{z}_i$ as $\theta$ increases from 0° to 20°, a result in reasonable agreement with the theoretical prediction.

In figure 8, our measurements of the dimensionless final height ($\tilde{z}_f = z_f M_o^{-1/4} N^{1/2}$)

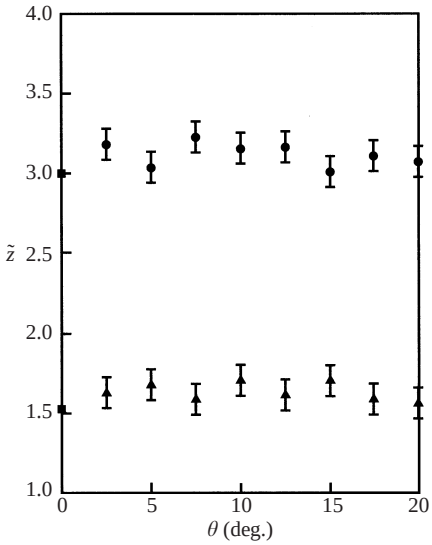


FIGURE 8. Dimensionless final (●) and spreading (▲) heights of a turbulent fountain in a stratified fluid as a function of the source inclination angle $\theta$. Also shown are mean heights for a vertical fountain (■), from Bloomfield & Kerr (1998).

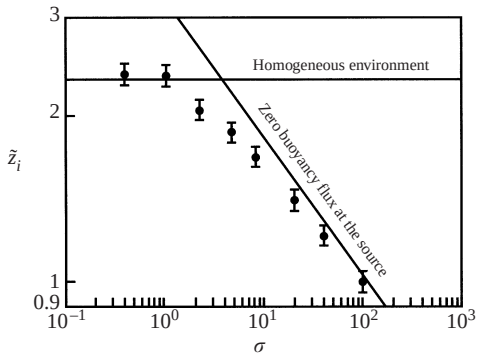


FIGURE 9. Dimensionless initial height of a turbulent fountain inclined at 10° to the vertical in a stratified fluid, as a function of $\sigma$. Also shown are the asymptotic behaviour of $\tilde{z}_i \to 2.32$ as $\sigma \to 0$ and $\tilde{z}_i \to 3.25\,\sigma^{-1/4}$ as $\sigma \to \infty$.

and the dimensionless spreading height ($\tilde{z}_s = z_s M_o^{-1/4} N^{1/2}$) are plotted against $\theta$. Although the variation in both $\tilde{z}_f$ and $\tilde{z}_s$ is small between 0° and 20°, there is some suggestion of a maximum in both heights (of about 3.15 and 1.67 respectively) at about 10°. The small variation with $\theta$ reflects both the weak effect of the decreasing vertical component of the source momentum flux (as is shown by the theoretical curve in figure 7) and the weak turbulent interaction between upflow and downflow when $\sigma = \infty$ (see figure 6*c* of Bloomfield & Kerr 1998).

### 3.3.2. *Non-zero buoyancy flux at the source*

For the general case of a non-zero buoyancy flux at the source, a total of eight experiments were performed at different values of $\sigma$, with the source at the (approximately optimal) angle of 10° to the vertical. The dimensionless initial and final heights ($\tilde{z}_i = z_i M_o^{-1/4} F_o^{1/2}$ and $\tilde{z}_f = z_f M_o^{-3/4} F_o^{1/2}$) are plotted against $\sigma$ in figures 9 and 10.

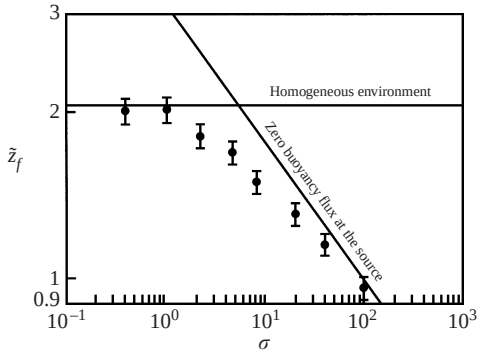


FIGURE 10. Dimensionless final height of a turbulent fountain inclined at 10° to the vertical in a stratified fluid, as a function of $\sigma$. Also shown are the asymptotic behaviour of $\tilde{z}_i \to 2.05$ as $\sigma \to 0$ and $\tilde{z}_i \to 3.15\,\sigma^{-1/4}$ as $\sigma \to \infty$.

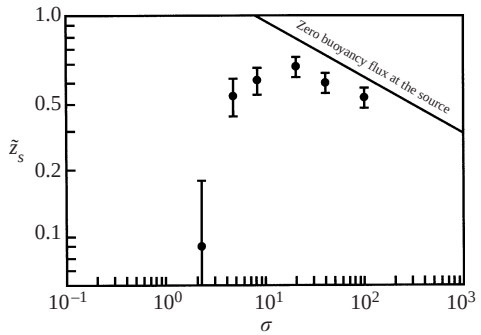


FIGURE 11. Dimensionless spreading height of a turbulent fountain inclined at 10° to the vertical in a stratified fluid, as a function of $\sigma$. Also shown is the asymptotic behaviour of $\tilde{z}_i \to 1.67\,\sigma^{-1/4}$ as $\sigma \to \infty$.

Also plotted are the limiting results for a homogeneous fluid ($\sigma = 0$) and for zero buoyancy flux at the source ($\sigma = \infty$). The experimental data approach within 5% of the homogeneous limit at $\sigma \approx 1.3$–$1.5$ and within 5% of the large-$\sigma$ limit at $\sigma \approx$ 60–70.

The effect of the ambient density gradient on the dimensionless spreading height ($\tilde{z}_s = z_s M_o^{-3/4} F_o^{1/2}$) is shown in figure 11. In a homogeneous environment the fountain fluid spreads at the base of the tank, and in a stratified environment the spreading height must again approach zero as $\sigma \to \infty$. Hence there is an intermediate value of the density gradient (at $\sigma_m \approx 20$) which gives a maximum in the dimensionless spreading height (of about 0.6). Also, there is a critical value $\sigma_c = 2.3 \pm 0.1$ that separates the regime where the fountain fluid spreads above the height of the source from the regime where the fluid spreads either below the height of the source or at the base of the tank. We note that the values of $\sigma_m$ and $\sigma_c$ for the inclined fountain are significantly smaller than the values (40–60 and $5.0 \pm 0.1$, respectively) found for a vertical fountain (Bloomfield & Kerr 1998), which is due to the greater height of rise and the greater mixing in the inclined fountain (cf. Baines *et al.* 1990).

## 4. Conclusions

We have presented an experimental investigation of the behaviour of inclined turbulent fountains in homogeneous and stratified environments. In a homogeneous environment, the initial fountain height was found to decrease monotonically as the inclination was increased, due primarily to the decreased vertical momentum of the source fluid. In contrast, the final fountain height was also affected by the turbulent interaction between the upflow and downflow, which decreased rapidly as the inclination was increased. As a result, the final height was found to increase, and then to decrease, as the inclination was increased. The maximum height of the fountain was found to occur at an angle of about 10°, at which point the fountain was about 20% higher than the height of a vertical fountain.

In exploring the behaviour of inclined turbulent fountains in a stratified environment, we first examined the limiting case of zero buoyancy flux at the source. We found that the effect of inclination angle on both the fountain and the spreading heights is small, although there is some suggestion of a maximum in both heights at about 10°. The small variation in this case was explained as being due to both the weak (1/4 power) dependence of the fountain height on the source momentum flux and the weak turbulent interaction between upflow and downflow. We then quantified the initial, final and spreading heights for a fountain inclined at 10°, as a function of the strength of the stratification in the environment. In terms of a dimensionless stratification parameter $\sigma$, the maximum spreading height was found to occur at $\sigma_m \approx 20$, while the transition from a positive to a zero (or negative) spreading height occurred at a critical value $\sigma_c = 2.3 \pm 0.1$.

As observed by Baines *et al.* (1990), an important industrial motivation for investigating inclined fountains is the increased penetration and mixing that can result for the same input momentum, energy or cost (or alternatively, the same penetration and mixing can be achieved for reduced energy or cost). From this study, we have shown that inclining a fountain in a homogeneous fluid by about 10° will produce the same penetration for about 22% less input momentum and about 39% less input energy. In addition, for engineering applications where the spreading height is important, we have shown that the spreading height is maximized when the stratification parameter $\sigma$ is about 20. Finally, for applications in which the finite extent of the environment is important, we note that it is straightforward to incorporate our current measurements for inclined fountains into existing models for fountain filling boxes in both homogeneous and stratified environments (Baines *et al.* 1990; Bloomfield & Kerr 1999).

We thank Tony Beasley, Melanie Cooper and Ross Wylde-Browne for their assistance with the laboratory experiments, and Stewart Turner and Graham Hughes for their helpful comments.

## REFERENCES

Baines, W. D., Turner, J. S. & Campbell, I. H. 1990 Turbulent fountains in an open chamber. *J. Fluid Mech.* **212**, 557–592.

Bloomfield, L. J. & Kerr, R. C. 1998 Turbulent fountains in a stratified fluid. *J. Fluid Mech.* **358**, 335–356.

Bloomfield, L. J. & Kerr, R. C. 1999 Turbulent fountains in a confined stratified fluid. *J. Fluid Mech.* **389**, 27–54.

Bloomfield, L. J. & Kerr, R. C. 2000 A theoretical model of a turbulent fountain. *J. Fluid Mech.* **424**, 197–216.

Campbell, I. H. & Turner, J. S. 1989 Fountains in magma chambers. *J. Petrol.* **30**, 885–923.

Fischer, H. B., List, E. J., Koh, R. C. Y., Imberger, J. & Brooks, N. H. 1979 *Mixing in Inland and Coastal Waters.* Academic.

Hofer, K. & Hutter, K. 1981*a* Turbulent jet diffusion in stratified, quiescent ambients. Part I: Theory. *J. Non.-Equil. Thermodyn.* **6**, 31–47.

Hofer, K. & Hutter, K. 1981*b* Turbulent jet diffusion in stratified, quiescent ambients. Part II: Experiments. *J. Non.-Equil. Thermodyn.* **6**, 49–64.

Koh, R. C. Y. & Brooks, N. H. 1975 Fluid mechanics of waste-water disposal in the ocean. *Annu. Rev. Fluid Mech.* **7**, 187–211.

Lane-Serff, G. F., Linden, P. F. & Hillel, M. 1993 Forced, angled plumes. *J. Hazardous Mat.* **33**, 75–99.

Larson, M. & Jönsson, L. 1994 Efficiency of mixing of a turbulent jet in a stably stratified fluid. *Proc. 4th Intl Symp. Stratified Flows, Grenoble, France* (ed. E. Hopfinger, B. Voisin & G. Chavand).

Lindberg, W. R. 1994 Experiments on negatively buoyant jets, with or without cross-flow. In *Recent Research Advances in the Fluid Mechanics of Turbulent Jets and Plumes* (ed. P. A. Davies & M. J. Valente Neves), pp. 131–145. Kluwer.

Lindberg, W. R. & Peterson, J. D. 1991 Negatively buoyant jet (or plume) with application to snowplow exit flow behaviour. *Transportation Research Record* **1304**, 219–229.

McClimans, T. & Eidnes, G. 2000 Forcing nutrients to the upper layer of a fjord by a buoyant plume. *Proc. 5th Intl. Symp. Stratified Flows, Vancouver, Canada*, pp. 199–204.

McDougall, T. J. 1981 Negatively buoyant vertical jets. *Tellus* **33**, 313–320.

Mizushina, T., Ogino, F., Takeuchi, H. & Ikawa, H. 1982 An experimental study of vertical turbulent jet with negative buoyancy. *Wärme-und Stoffübertragung* **16**, 15–21. **5**, 151–163.

Morton, B. R., Taylor, G. I. & Turner, J. S. 1956 Turbulent gravitational convection from maintained and instantaneous sources. *Proc. R. Soc. Lond.* A **234**, 1–23.

Oster, G. 1965 Density gradients. *Sci. Am.* **213**, 70–76.

Schatzmann, M. 1978 The integral equations for round buoyant jets in stratified flows. *J. Angew. Math. Phys.* **29**, 608–630.

Turner, J. S. 1966 Jets and plumes with negative or reversing buoyancy. *J. Fluid Mech.* **26**, 779–792.

Turner, J. S. 1973 *Buoyancy Effects in Fluids.* Cambridge University Press.

Turner, J. S. & Campbell, I. H. 1986 Convection and mixing in magma chambers. *Earth Sci. Rev.* **23**, 255–352.

Woods, A. W. & Caulfield, C. P. 1992 A laboratory study of explosive volcanic eruptions. *J. Geophys. Res.* **97**, 6699–6712.